THE ASTROPHYSICAL JOURNAL, 412:612–617, 1993 August 1

ABUNDANCE INHOMOGENEITIES AND ATMOSPHERIC STRUCTURE IN CN-BIMODAL GLOBULAR CLUSTER GIANTS

JEREMY J. DRAKE,[1,2] BERTRAND PLEZ,[1] AND VERNE V. SMITH[1]
Received 1992 December 7; accepted 1993 February 9

ABSTRACT

It has been suggested by several authors that the sodium and aluminium abundance variations correlating with CN-band strength, frequently observed in CN-bimodal globular cluster giants, could be spurious manifestations of different temperature structures in the "CN-strong" and "CN-weak" stars, caused by different molecular line blanketing related to the C, N, and O trio. For stellar parameters generally appropriate to giants in the intermediate metallicity CN-bimodal cluster M4, we demonstrate through new model atmosphere calculations, employing opacity sampling and spherical geometry, that the observed abundance anomalies cannot be the result of atmospheric temperature structure. Our results using spherical geometry are compared to identical calculations performed with plane-parallel geometry: the effects of atmospheric extension on derived abundances for all lines considered amount to less than 0.1 dex.

Subject headings: globular clusters: general — stars: abundances — stars: atmospheres — stars: evolution — stars: giant

1. INTRODUCTION

The origins of the now well-documented abundance inhomogeneities exhibited by stars within globular clusters remains a controversial topic; see Smith (1987, 1989), Pilachowski (1989), and Suntzeff (1989) for recent reviews. One of the most striking aspects of the puzzle is the bimodal distribution of CN molecular band strengths observed in many of the intermediate metallicity globular clusters ($-0.7 \geq [M/H] \geq -1.6$). The last decade has witnessed a deepening of this mystery, with a growing body of evidence suggesting that the enhanced CN-bands are often accompanied by enhancements in Na I and Al I line strength (Peterson 1980; Cottrell & DaCosta 1981; Norris et al. 1981; Lloyd Evans, Menzies, & Smith 1982; Norris & Smith 1983; Norris & Pilachowski 1985; Lehnert, Bell, & Cohen 1991; Smith & Wirth 1991; Drake, Smith, & Suntzeff 1992). If such line strength variations correspond to real Na and Al abundance differences in the "CN-strong" and "CN-weak" stars, then these abundances would provide key constraints for theories attempting to explain the abundance inhomogeneities.

There are two basic scenarios through which the cluster abundance inhomogeneities could arise; see, e.g., Smith (1987), Smith & Wirth (1991), and Suntzeff & Smith (1991) for more complete discussions. Briefly, in one scenario, often referred to as the "Mixing Hypothesis," it is postulated that the abundance anomalies are the natural consequence of dredge-up of material processed by interior nucleosynthesis (e.g., Sweigart & Mengel 1979). In the second, the inhomogeneities could arise through contamination, either prior to the formation of the cluster stars, by primordial proto-cluster abundance inhomogeneities; or during the life of the stars, by accretion of chemically enriched material. In order to explain enhancements of Na and Al, the Mixing Hypothesis would require heterodox stellar evolution theory, since canonical stellar models do not predict the abundances of these two elements to change on the surface of a low-mass star as a result of dredge-up (e.g., Iben & Renzini 1983). Contamination of the cluster stars by material external to themselves, either prior to their formation or during their evolution, would require the contaminant to be enriched in Na and Al, but not in the other elements which are observed to be homogeneously distributed. This criterion severely limits the possible origins of such material—see, e.g., Smith & Wirth (1991) and Suntzeff & Smith (1991) for recent discussions.

Despite the pivotal role Na and Al might play in the resolution of the enigma, the question of whether the observed line enhancements correspond to real Na and Al abundance differences remains controversial. Several authors (e.g., Peterson 1976; Cohen 1978; Peterson 1980; Norris & Smith 1983; Norris & Pilachowski 1985; Pilachowski 1989; Smith 1987, 1989; Smith & Wirth 1991) have suggested two potential obstacles to a straightforward interpretation in terms of abundance variations: (1) departures from LTE; (2) differences in atmospheric temperature structure in the CN-strong and CN-weak stars, caused by the different C-, N-, and O-related molecular line blanketing.

Non-LTE effects alone would seem an improbable explanation for the line strength differences, since many authors have now observed equivalent width variations in lines due to weak, nonresonance transitions in stars with very similar temperatures and luminosities (e.g., Cottrell & Da Costa 1981; Pilachowski 1989; Lehnert et al. 1991; Smith & Wirth 1991; Drake et al. 1992; Kraft et al. 1993). Drake et al. (1992) presented abundances based on the weak Na lines of multiplet 5 near λ6160 which differ by 0.3 dex between CN-strong and CN-weak giants in the CN-bimodal cluster M4. They ruled out any significance of non-LTE effects, describing the results of detailed non-LTE calculations for Na which suggested that relaxing the LTE assumption erodes the Na abundance difference by only 0.02 dex.

A good indication that the second of the above "obstacles"—atmospheric temperature structure differences due to molecular blanketing—is not significant was given by Campbell & Smith (1987). Line blanketing affects both the deep atmospheric layers through backwarming, and the higher layers through, e.g., surface cooling—see Gustafsson et al.

[1] Astronomy Department, University of Texas at Austin, Austin TX 78712.
[2] Center for EUV Astrophysics, University of California, 2150 Kittredge Street, Berkeley, CA 94720.

(1975) and Carbon (1979) for lucid discussions. Thus even weak lines formed in deep photospheric layers might potentially be affected by differences in line blanketing. Campbell and Smith argued that the λ7699 K I resonance line should also be sensitive to the same structure effects as the lines of Na I and Al I which are observed to be correlated with CN-band strength. They observed the λ7699 K I line in a total of 13 stars in the globular clusters M4, 47 Tuc and NGC 6752, along with lines due to Na, Al and several other species, and found no significant variation in K line strength between CN-strong and CN-weak stars. They concluded that there were no significant atmospheric structure differences between CN-rich and CN-poor globular cluster giants. While fairly convincing, there is still some room for doubt in this conclusion. The K I λ7699 line is both significantly stronger than the weak Na I and Al I subordinate lines and weaker than the Na and Al resonance lines, and, furthermore, the continuous absorption coefficient gradually increases toward the near infrared, tending to move the depth of line formation higher toward longer wavelengths: in short, the K I line samples a different range of atmospheric depth than the Na and Al lines at shorter wavelengths. Different atmospheric structures in the CN-weak and -strong stars might not then affect the K, Na, and Al lines in exactly the same fashion, and the result of Campbell & Smith (1987), while a good indicator of the insignificance of atmospheric structure variations, is not a definitive test. The problem still awaits a more rigorous theoretical model atmosphere investigation.

In this paper, we present the results of new opacity sampling spherical model atmosphere calculations, employing recent molecular and atomic line data (Plez, Brett, & Nordlund 1992). A grid of models representing typical CN-strong and CN-weak intermediate metallicity globular cluster giants have been computed. These have been used to calculate the effects of the different C-, N-, and O-related molecular blanketing in the CN-strong and CN-weak stars on spectroscopic measurements of Na, Al, Ca, and Fe abundances. We demonstrate conclusively that atmospheric temperature structure effects are not responsible for the abundance variations commonly observed in CN-bimodal globular clusters. Our calculations also enable us to estimate the effects of atmospheric extension on globular cluster abundance measurements. We show that the differences between abundances derived in plane parallel and spherical geometries are likely to be less than 0.1 dex.

2. METHOD

2.1. *Model Atmospheres*

In order to investigate the possible effects of differential molecular blanketing on atmospheric temperature structure, we have calculated models for two different sets of C, N, and O abundances typical of those found in CN-strong and CN-weak giants of the intermediate metallicity bimodal globular clusters. Note that the atomic and ionic line blanketing, which is dominated by the iron group species, is not affected directly by these elements, which all exhibit relatively sparse line spectra. Iron group species are generally observed to be homogeneously distributed in CN-bimodal clusters (e.g., see Smith 1987), and so the only influence of C, N, and O abundance variations on the atomic and ionic line blanketing will be through any changes in atmospheric structure resulting from molecular blanketing variations.

Our model atmosphere code, SOSMARCS, is derived from the MARCS suite of programs originally developed by Gustafsson et al. (1975), and subsequently has been updated to include the effects of spherical geometry and to calculate the effects of line blanketing using opacity sampling techniques (Plez et al. 1992). As a test, we also calculated some models in plane-parallel geometry using the same code, in order to estimate the influence of atmospheric extension on the derived abundances. Whilst "traditional" MARCS models, or models adopted from the grid of MARCS models published by Bell et al. (1976), have long been the model atmosphere mainstay of globular cluster abundance studies, these have been computed using opacity distribution functions (ODFs) calculated for limited, fixed patterns of C, N, and O abundances. Using such models, it is not possible to account rigorously in the model structure for a chemical composition which differs from that for which the limited set of ODFs was calculated. The opacity sampling approach circumvents this restriction by explicitly calculating the line and continuous opacity for any given composition. The nemesis of this method is that a sufficiently large number of frequency points to provide an accurate sampling of the stellar flux is required. In previous years the problem was tractable using only the most powerful computers. However, the rapid evolution of computer hardware in recent years has now reduced this quasi-intractable problem to one of relatively modest computational effort.

The C, N, and O abundances, together with the atmospheric parameters $T_{\rm eff}$, log g, and metallicity (represented here by the abundance of iron relative to the solar value, [Fe/H]), that we adopted for the model atmosphere calculations are listed in Table 1. We chose to adopt atmospheric parameters and abundances which were close to those found from recent studies of giants in the CN-bimodal globular cluster M4: atmospheric parameters were taken from Drake et al. (1993), C and N abundances were taken from Suntzeff & Smith (1991), and the O abundances were taken from Drake et al. (1992). Drake et al. found the iron abundance of M4 to be very close to [Fe/H] = -1. However, in order to probe the differential effects of molecular blanketing down to lower metallicities, we also calculated the same set of models with all abundances reduced by 0.5 dex (i.e., scaled to [Fe/H] = -1.5). In the case of M4, Drake et al. found the abundance of Ca, an α-element, to be enhanced relative to Fe by $+0.25$ dex. It is likely that the abundances of the other α-elements, including Mg and Si (which are a major source of electrons in late-type stellar photospheres) are also enhanced relative to Fe by a similar

TABLE 1

THE ATMOSPHERIC PARAMETERS AND C, N, AND O ABUNDANCES ADOPTED FOR THE MODEL ATMOSPHERE CALCULATIONS[a]

$T_{\rm eff}$, log g	[Fe/H]	C/H	N/H	O/H	Geometry[b]	Code
4400, 1.3....	-1.0	6.60	7.60	8.10	Sph	44S10S
		7.10	7.10	8.30	Sph	44W10S
		7.10	7.10	8.30	PP	44W10P
	-1.5	6.10	7.10	7.60	Sph	44S15S
		6.60	6.60	7.80	Sph	44W15S
3900, 0.8....	-1.0	6.60	7.60	8.10	Sph	39S10S
		7.10	7.10	8.30	Sph	39W10S
		7.10	7.10	8.30	PP	39W10P
	-1.5	6.10	7.10	7.60	Sph	39S15S
		6.60	6.60	7.80	Sph	39W15S

[a] The abundances with respect to Fe abundance, relative to solar, adopted for the α-elements was [α/Fe] = $+0.25$.

[b] Spherical and plane-parallel geometries are indicated by the abbreviations "Sph" and "PP," respectively.

amount (e.g., see Wheeler, Sneden, & Truran 1989), and we have therefore adopted abundances relative to Fe for these elements equivalent to $[\alpha/\mathrm{Fe}] = +0.25$.

For the spherically symmetric models an additional parameter is required. We chose $M/M_{\odot} = 0.8$ for both series of models, which leads to $M_{\mathrm{bol}} = -1.67$ for the $T_{\mathrm{eff}} = 4400$ K models and $M_{\mathrm{bol}} = -2.40$ for the $T_{\mathrm{eff}} = 3900$ K models.

2.2. *Abundances*

We considered the elements Na, Al, O, Ca, and Fe. Our method, in essence, involved calculating abundances for these elements from given "observed" equivalent widths for each of the model atmospheres in our grid. Whilst Na and Al are commonly seen to vary between CN-strong and CN-weak stars, Fe and Ca are generally observed to be homogeneously distributed, within experimental uncertainties, in the intermediate metallicity CN-bimodal clusters (e.g., Smith 1987). If line blanketing effects do induce significant changes in theoretical Na and Al line strengths calculated for the CN-strong and CN-weak star models, then we would not expect to see similarly large changes in Ca and Fe lines. These latter elements, then, serve as a control.

In the case of Na, we considered the multiplet 5 lines at λ6154 and λ6160, the λ5683 line of multiplet 6, the near infrared line of multiplet 4 at λ8183, and the D line at λ5890. The only Al lines considered were the lines of multiplet 5 at λ6696 and λ6698: since both lines of this multiplet are observable down to metallicities of $[\mathrm{Fe/H}] = -1.5$, they are favored over the resonance lines, which are blended with the wings of the Ca II H and K lines and numerous other spectral features. The most useful Ca I lines in late-type stellar spectra for abundance analyses are those near 2.5 eV excitation, for which Smith and coworkers have derived a fairly extensive set of atomic data (Smith & O'Neill 1975; Smith 1981; Smith & Raggett 1981). For this study we have chosen three of these lines, which cover a range in line strength. In the case of Fe, we have considered weak and moderately strong Fe I lines of high excitation, a low-excitation line of medium strength, and a typical line of Fe II. All of these lines, and their germane atomic data, are listed in Table 2. Oscillator strengths were adopted from: Wiese & Martin (1980) (Na); Lambert & Luck (1978) (O); Smith (1981) (Ca). In the case of the Fe I, Fe II, and Al I lines, oscillator strengths are from Drake et al. (1993); these were calculated from the solar flux spectrum (Kurucz et al. 1984) using the Holweger & Müller (1974) solar model, a microturbulence of $\xi = 1.5$ km s^{-1} (Smith 1981), and Fe and Al abundances of 7.50 and 6.49, respectively. The only collision broadening parameter (here expressed as $-\log C_6$) of significance is that for the Na resonance line. This was taken from Smith et al. (1985). Values for Ca are from Smith (1981), and the remainder were derived using the Unsöld (1955) relation and orbital mean-square-radii from the Coulomb approximation (Na, Al, Fe II) and from Warner (1969) (Fe I), with enhancement factors of between 1 and 2. We emphasize that our choice of atomic data is not critical to the analysis.

For our set of lines, we calculated equivalent widths in the LTE approximation using the spherical, CN-weak models at each temperature and global metallicity of our grid: adopting the model abreviations listed in Table 1, these models were 44W10S, 39W10S, 44W15S, and 39W15S. These equivalent widths then served as our "observed" equivalent widths, from which we calculated abundances for the remaining models in the grid.

3. RESULTS AND DISCUSSION

3.1. *Model Atmospheres*

3.1.1. *Molecular Blanketing*

The temperature structures, $T(\tau_{\mathrm{Ross}})$, for all of the models in our grid are illustrated in Figures 1*a* and 1*b*. From Figure 1*a* it can be seen immediately that the differences in temperature structure between the various models are not large.

Turning first toward the deep layers, the obvious effect here is that of metallicity: the more metal-deficient models,

TABLE 2

LINES STUDIED, WITH THE ABUNDANCES ADOPTED FOR EACH ELEMENT, AND EQUIVALENT WIDTHS

SPECIES	$[A/\mathrm{Fe}]$[a] MULT	λ (Å)	ξ (eV)	log gf	$-\log C_6$	EQUIVALENT WIDTH (mÅ)[b] 44W10S	39W10S	44W15S	39W15S
Na I	+0.15								
	6	5682.663	2.10	−0.70	29.73	91	117	57	88
	1	5889.953	0.00	0.117	30.49	704	1675	481	1033
	5	6154.230	2.10	−1.56	29.77	37	67	14	34
	5	6160.753	2.10	−1.26	29.77	56	88	26	53
	4	8183.256	2.09	0.220	29.97	174	206	138	176
Al I	+0.50								
	5	6696.032	3.13	−1.461	30.46	60	88	30	55
	5	6698.669	3.13	−1.803	30.46	39	65	16	33
O I	+0.30								
	1 F	6300.311	0.00	−9.75	30.0	54	80	33	55
Fe I	0.0								
	1180	5862.370	4.55	−0.390	30.26	78	79	54	60
	1086	5814.814	4.26	−1.818	30.52	25	30	10	15
	62	6173.341	2.22	−2.95	31.24	109	124	87	108
Fe II	0.0								
	74	6456.387	3.89	−2.328	31.16	43	22	32	17
Ca I	+0.25								
	20	6166.44	2.51	−1.142	29.69	98	128	69	103
	18	6439.07	2.51	0.390	30.80	188	233	160	193

[a] Abundances with respect to their solar values, relative to iron, $[A/\mathrm{Fe}]$.
[b] Equivalent widths calculated using the set of CN-weak models (see text).

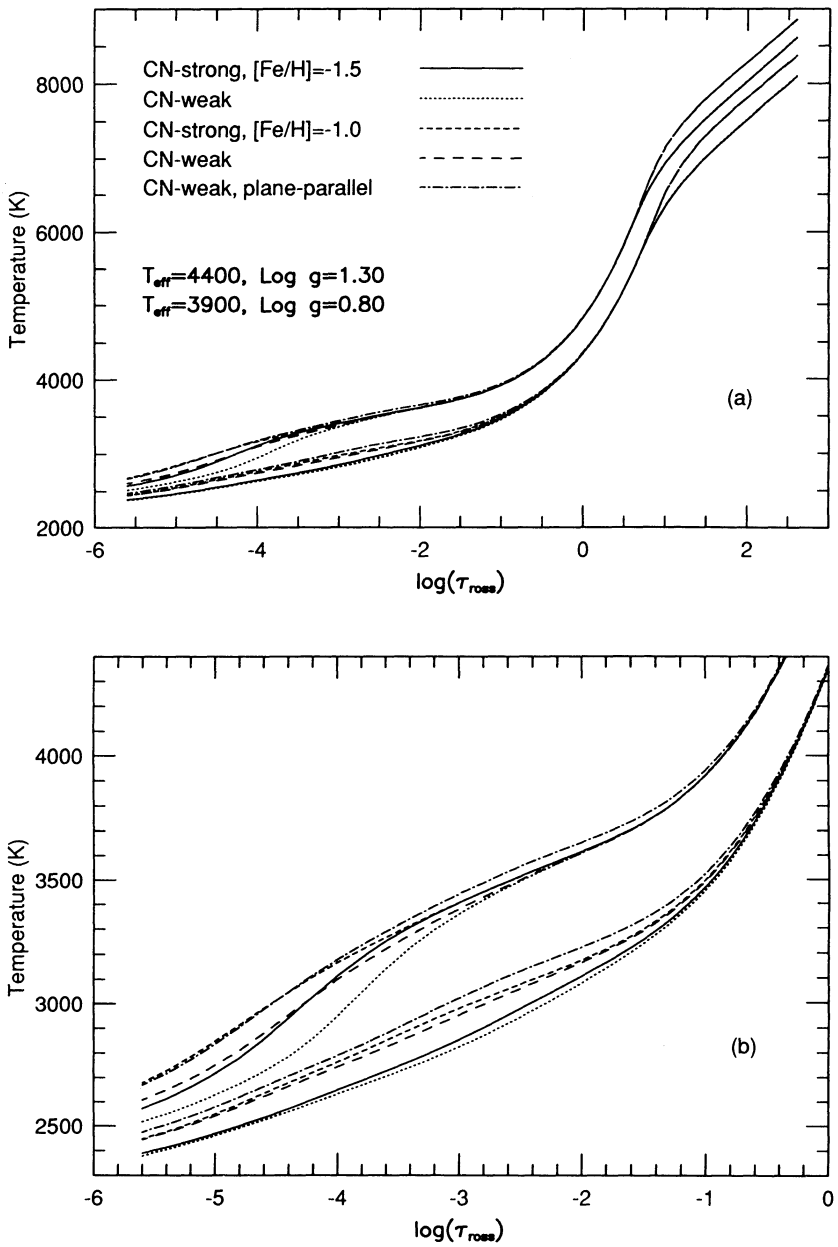

FIG. 1.—(*a*) Atmospheric temperature structures of the different models of the grid; (*b*) details of the model structures above log $\tau_{\rm Ross} = 0$.

[Fe/H] = −1.50, are ∼300 K cooler than the [Fe/H] = −1.0 models in the deepest layers. This result is a direct consequence of the greater efficiency of convection in the more metal-poor models. As the metallicity of the model is decreased, the ionization zone moves outwards because of the depletion in electron density, and the convective flux reaches closer to the surface, which leads generally to a more shallow temperature gradient in these layers—see Gustafsson et al. (1975) for a more complete discussion. The onset of line formation is typically above log $\tau = 1$; therefore, these layers have little effect on derived abundances.

All of the models have nearly identical temperature structures at log $\tau_{\rm Ross} = 0$, but they begin to differ toward the higher layers (Fig. 1*b*). In the case of the spherical models, the temperatures toward the outer layers are controlled to a large extent by a complex interplay of heating and cooling by CO, H_2O, and TiO line opacities. In general, CO and H_2O cool down the outer layers (see e.g., Gustafsson et al. 1975; Auman 1969), while TiO has a heating effect (see Krupp, Collins, & Johnson 1978). The CN itself tends to have a backwarming effect, but the impact on the model structure is less significant. The CN-weak models are all cooler in the outer layers than the CN-strong models, primarily because of CO: these models have higher C abundances, slightly higher O abundances, and consequently stronger CO bands and more cooling through CO lines. This anticorrelation of CO and CN band strengths is in keeping with observations—see, for example, the CO photometry for M4 from Frogel, Persson, & Cohen (1983) and the CN-strength measurements of Norris (1981) and Suntzeff & Smith (1991). Heating by TiO and cooling by water vapor can partly cancel one another, with the balance tending toward a net cooling effect in favor of H_2O, as shown by our calculations

of models without TiO opacity. This reflects the growing importance of water opacity relative to TiO or CO at lower metallicities.

The maximum temperature difference in the outer layers between CN-weak and CN-strong models for $T_{\rm eff} = 4400$ K amounts to approximately 150 K at $\log \tau_{\rm Ross} \sim -4$ for [Fe/H] $= -1.5$, and to about half of this for [Fe/H] $= -1.0$. For $T_{\rm eff} = 3900$ K, the effects are much smaller, amounting to less than 50 K for both metallicities.

3.1.2. *Spherical versus Plane-Parallel*

The effects of extension on atmospheric structure have been discussed in detail by previous authors (Schmid-Burgk & Scholz 1975; Watanabe & Kodaira 1978, 1979; Scholz & Wehrse 1982; Bessell et al. 1989; Plez 1990). In brief, the radiation field in a spherical model becomes diluted with increasing height, an effect which is not accounted for in a plane-parallel model. The result of this is a general lowering of the temperature in the outer layers relative to the plane-parallel case. Our results reflect these effects, the plane-parallel models (CN-weak and [Fe/H] $= -1.0$) for both effective temperatures being hotter than their spherical counterparts towards the higher layers. The models begin to diverge near $\log \tau_{\rm ross} = -1$, above which point the plane-parallel case remains 50–75 K hotter. In spherical symmetry, decreasing gravity with increasing radius also leads to lower gas pressure in higher atmospheric regions, although in general this has a much less significant effect on the derivation of element abundances.

3.2. *Abundances*

3.2.1. *Molecular Blanketing*

Our results, represented by the abundance differences, $\Delta \log A$ (defined as the quantity $\log A_{\rm CN\text{-}strong} - \log A_{\rm CN\text{-}weak}$), arising as a result of using the models with different C, N, and O abundances, are illustrated in Figure 2. We point out two singularly important aspects of these results: (1) the differences between abundances derived using CN-strong and CN-weak models are all very small for both temperatures and metallicities considered; (2) Fe and Ca lines—our "control" lines—are affected to a similar extent as the lines of Na and Al.

In the case of the hotter models ($T_{\rm eff} = 4400$ K), there is an obvious trend in $\Delta \log A$ with line strength: differences are small for weak lines on the linear part of the curve of growth, they reach a maximum for medium-strength lines lying on the flat part of the curve, and then they drop again for the strong Na D line. This result is simply a reflection of the depths of formation of the different strength lines. Very generally, weak lines are formed mostly in a relatively narrow region in the atmosphere around $\log \tau = 0$ (e.g., see Fig. 2 of Drake et al. 1992)—mostly above the region where the different model temperature structures diverge. Stronger lines nearing saturation form a greater fraction of their equivalent widths in higher layers, where our CN-weak and CN-strong atmospheres have different temperature structures. Growth in the equivalent widths of very strong lines (e.g., the Na D lines) occurs predominantly in the development of collisionally broadened wings, which again takes place in the deeper layers of the atmosphere, below the region affected by the different molecular blanketing.

In the case of the cooler models, the difference between the CN-weak and CN-strong temperature structures is so small that none of the lines are significantly affected. A small residual curve-of-growth effect is visible, with a peak in abundance difference, excluding the Fe II line, occurring near $\log (W/\lambda) = -4.5$. Note that the abundance difference for the Fe II line is positive, rather than negative. This is due to a slight difference in pressure at line formation depths between the two models, which noticeably affects a minor species such as Fe II through the ionization equilibrium.

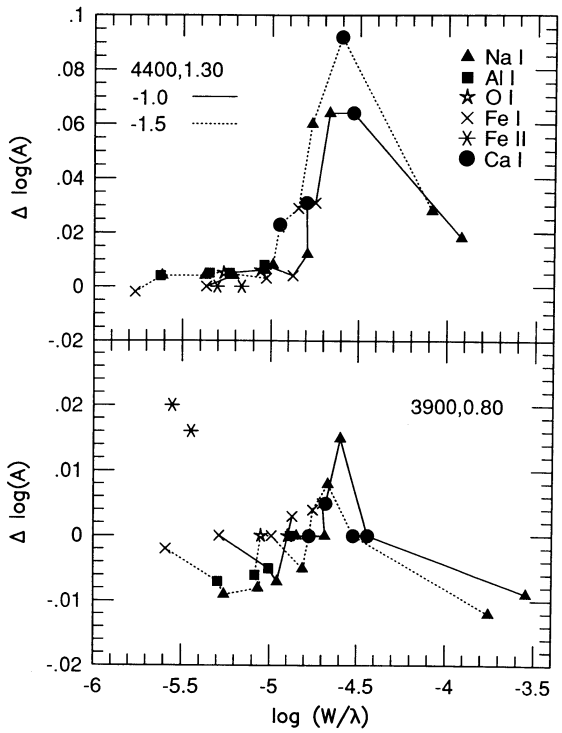

FIG. 2.—Differences in abundances, $\Delta \log A$, derived using the CN-strong and CN-weak models, as defined in the text. The solid and dashed lines serve to separate the points corresponding to models with metallicities [M/H] $= -1.0$ and -1.5, respectively, and to highlight the dependence of $\Delta \log A$ on equivalent width; points corresponding to Fe II lines are not joined to those due to neutral species because of their different behavior to the changes in model structure.

3.2.2. *Spherical versus Plane-Parallel*

The effects of neglecting spherical geometry are illustrated in Figure 3 and are tabulated for a subset of our lines in Table 3. Here, $\Delta \log A$ is defined as the quantity $\log A_{\rm PP} - \log A_{\rm Sph}$, with the subscripts "PP" and "Sph" having their obvious meanings. The plane-parallel models are hotter than the corresponding spherical models in the regions of line formation, and consequently lines due to neutral species yield larger

TABLE 3

THE DIFFERENCES, $\Delta \log A$, BETWEEN ABUNDANCES DERIVED USING PLANE-PARALLEL AND SPHERICAL GEOMETRIES FOR SELECTED LINES

SPECIES	λ(Å)	eV	$\Delta \log A$[a] 4400, 1.3	$\Delta \log A$[a] 3900, 0.8
Na I	5889.953	0.00	+0.069	+0.095
	6154.230	2.10	+0.040	+0.055
Al I	6696.032	3.13	+0.040	+0.050
O I	6300.311	0.00	+0.013	+0.023
Ca I	6439.07	2.51	+0.066	+0.059
Fe I	6173.341	2.22	+0.086	+0.025
Fe II	6456.387	3.89	−0.043	−0.055

[a] Positive values indicate that a larger abundance is derived using plane-parallel models.

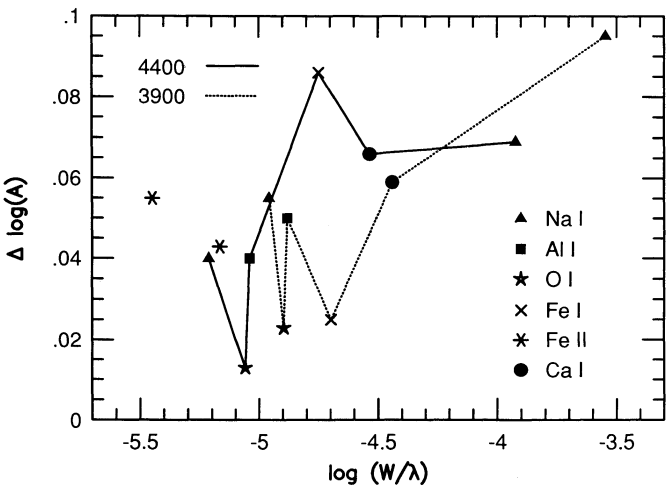

FIG. 3.—Differences in abundances, Δ log A, derived using the CN-weak spherical and plane-parallel models, as defined in the text. For convenience, Δ log A for the Fe II line is illustrated with the opposite sign (see Table 3).

abundances under the assumption of plane-parallel geometry, while lines due to ionized species will in general yield smaller abundances. These effects are larger than those due to differential molecular blanketing—a consequence of the temperature structures of the spherical and plane-parallel models diverging at greater optical depth than those of the spherical models with different blanketing. This is also reflected in the (opposite) effect for the Fe II λ6456 line, whose mean depth of formation is slightly greater than those of the neutral species. Again the magnitude of the effect is seen to depend on the line position on the curve of growth.

These are encouraging results for conventional, plane-parallel model atmosphere analyses of globular cluster giants: for none of our lines do we find the effects of atmospheric extension to be greater than 0.1 dex—significantly smaller than the errors intrinsic to the majority of the abundance analyses themselves. In an earlier study, Plez (1990) found effects of the same order of magnitude for, e.g., CO and CN lines in the range 3500 K < $T_{\rm eff}$ < 4500 K.

4. CONCLUSIONS

We have demonstrated, using the latest spherical model atmospheres, that the effects of different molecular line blanketing on the temperature structures of typical CN-strong and CN-weak intermediate metallicity CN-bimodal globular cluster giants are small. These results confirm the empirical deduction of Campbell & Smith (1987). Consequently, none of the abundance anomalies or line strength differences reported for CN-bimodal globular clusters can be attributed to atmospheric structure effects.

The effects of neglecting spherical geometry in these spectral types are relatively small, although somewhat larger than the effects of the different molecular blanketing. The spherical models are typically cooler in the outer layers as a result of dilution of the radiation field caused by extension. For neutral species, the resulting difference in abundances calculated for plane-parallel and spherical geometry generally amount to some 0.05 dex for weak lines, and up to 0.1 dex for stronger lines, depending on the location of the line on the curve of growth, in the sense that the plane-parallel models yield the larger values. For the Fe II line considered here, the geometrical effects amounted to approximately 0.05 dex, with the opposite sign.

We would like to extend warm thanks to Prof. J. Norris (Mount Stromlo & Siding Spring Observatories), whose pertinent comments partly inspired this work. J. J. D was supported by a NATO Postdoctoral Fellowship during the course of this work, and in the final stages by NASA contract NAS5-30180, administered by the Center for EUV Astrophysics at UC Berkeley. J. J. D. thanks the Principal Investigator, Stuart Bowyer, and the *EUVE* science team for their advice and support. B. P. and V. V. S. were supported in part by the NSF (AST 91-15090) and the Robert A. Welch foundation of Houston, Texas.

REFERENCES

Auman, J. R. 1969, ApJ, 157, 799
Bell, R. A., Eriksson, K., Gustafsson, G., & Nordlund, Å. 1976, A&AS, 23, 37
Bessell, M. S., Brett, J. M., Scholz, M., & Wood, P. R. 1989, A&AS, 77, 1
Campbell, B., & Smith, G. H. 1987, ApJ, 323, L69
Carbon, D. F. 1979, ARA&A, 17, 513
Cohen, J. G. 1978, ApJ, 223, 487
Cottrell, P. L., & Da Costa, G. S. 1981, ApJ, 245, L79
Drake, J. J., Smith, V. V., & Suntzeff, N. B. 1992, ApJ, 395, L95
———. 1993, in preparation
Frogel, J. A., Persson, S. E., & Cohen, J. G. 1983, ApJS, 53, 713
Gustafsson, B., Bell, R. A., Eriksson, K., & Nordlund, Å. 1975, A&A, 42, 407
Holweger, H., & Müller, E. 1974, Sol. Phys., 39, 19
Iben, I., Jr., & Renzini, A. 1983, ARA&A, 21, 271
Kraft, R. P., Sneden, C., Langer, G. E., & Prosser, C. F. 1993, ApJ, in press
Krupp, B., Collins, J. G., & Johnson, H. R. 1978, ApJ, 219, 963
Kurucz, R. L., Furenlid, I., Brault, J. W., & Testerman, L. 1984, Solar Flux Atlas from 596 to 1300 nm, National Solar Observatory Atlas No. 1 (Tucson: NSO)
Lambert, D. L., & Luck, R. E. 1978, MNRAS, 183, 79
Lehnert, M. D., Bell, R. A., & Cohen, J. G. 1991, ApJ, 367, 514
Lloyd Evans, T., Menzies, J. W., & Smith, G. H. 1982, MNRAS, 201, 137
Norris, J. 1981, ApJ, 248, 177
Norris, J., Cottrell, P. L., Freeman, K. C., & Da Costa, G. S. 1981, ApJ, 244, 205
Norris, J., & Pilachowski, C. A. 1985, ApJ, 299, 295
Norris, J., & Smith, G. H. 1983, ApJ, 272, 635
Peterson, R. C. 1976, ApJS, 30, 61
———. 1980, ApJ, 237, L87
Pilachowski, C. A. 1989, in IAU General Assembly 20, The Abundance Spread within Globular Clusters: Spectroscopy of Individual Stars, ed. G. Cayrel de Strobel, M. Spite, & T. Lloyd Evans (Paris: Obs. Paris), 1
Plez, B. 1990, Mem. Soc. Astron. Ital., 61 (3), 765
Plez, B., Brett, J. M., & Nordlund, Å. 1992, A&A, 256, 551
Schmid-Burgk, J., & Scholz, M. 1975, A&A, 41, 41
Scholz, M., & Wehrse, R. 1982, MNRAS, 200, 41
Smith, G. 1981, A&A, 103, 351
Smith, G., Monteiro, T. S., Dickinson, A. S., & Lewis, E. L. 1985, MNRAS, 217, 679
Smith, G., & O'Neill, J. A. 1975, A&A, 38, 1
Smith, G., Raggett, D. St. J. 1981, J. Phys. B, 14, 4015
Smith, G. H. 1987, PASP, 99, 67
———. 1989, in IAU General Assembly 20, The Abundance Spread of Globular Clusters: Spectroscopy of Individual Stars, ed. G. Cayrel de Strobel, M. Spite, & T. Lloyd Evans (Paris: Obs. Paris), 63
Smith, G. H., & Wirth, G. D. 1991, PASP, 103, 1158
Suntzeff, N. B. 1989, in IAU General Assembly 20, The Abundance Spread of Globular Clusters: Spectroscopy of Individual Stars, ed. G. Cayrel de Strobel, M. Spite, & T. Lloyd Evans (Paris: Obs. Paris), 71
Suntzeff, N. B., & Smith, V. V. 1991, ApJ, 381, 160
Sweigart, A. V., & Mengel, J. G. 1979, ApJ, 229, 624
Unsöld, A. 1955, Physik der Sternatmosphären (Berlin: Springer)
Warner, B. 1969, MNRAS, 136, 381
Watanabe, T., & Kodaira, K. 1978, PASJ, 30, 21
———. 1979, PASJ, 31, 61
Wheeler, J. C., Sneden, C., & Truran, J. W. 1989, ARA&A, 27, 279
Wiese, W. L., & Martin, G. A. 1980, Wavelengths and Transition Probabilities for Atoms and Atomic Ions, NSRDS–NBS 68, Vol. 2